Hindawi Publishing Corporation
Journal of Electrical and Computer Engineering
Volume 2012, Article ID 139416, 16 pages
doi:10.1155/2012/139416

Research Article

Compensation of Linear Multiscale Doppler for OFDM-Based Underwater Acoustic Communication Systems

A. E. Abdelkareem, B. S. Sharif, C. C. Tsimenidis, and J. A. Neasham

School of Electrical and Electronic Engineering, Newcastle University, Newcastle upon Tyne NE1 7RU, UK

Correspondence should be addressed to A. E. Abdelkareem, a.e.abdelkareem@ncl.ac.uk

Received 21 February 2012; Accepted 21 May 2012

Academic Editor: Yuriy Zakharov

In particular cases, such as acceleration, it is required to design a receiver structure that is capable of accomplishing time varying Doppler compensation. In this paper, two approaches are taken into consideration in order to estimate the symbol timing offset parameter. The first method employed to achieve an estimate of this particular parameter is based upon centroid localization and this prediction is reinforced by a second technique which utilises linear prediction, based on the assumption that the speed changes linearly during the OFDM symbol time. Subsequently, the two estimations of the symbol timing offset parameter are smoothed in order to obtain a fine tuned approximation of the Doppler scale. Additionally, the effects of weighting coefficients on smoothing the Doppler scale and on the performance of the receiver are also investigated. The proposed receiver is investigated, incorporating an improvement that includes fine tuning of the coarse timing synchronization in order to accommodate the time-varying Doppler. Based on this fine-tuned timing synchronization, an extension to the improved receiver is presented to assess the performance of two point correlations. The proposed algorithms' performances were investigated using real data obtained from an experiment that took place in the North Sea in 2009.

1. Introduction

Several time-domain receivers that adopt coherent modulation with an emphasis on channel equalization in order to increase communication reliability have been suggested. However, the time-varying doubly-spread characteristic of the underwater acoustic (UWA) channel requires a highly complex equalizer. Recently, an alternative low-complexity, high-speed multicarrier communication system, in the form of OFDM, has attracted considerable interest in the field of underwater acoustic communication (UWAC). This is mainly due to its simplicity of operation by means of the fast Fourier transform (FFT) for the purpose of modulation/demodulation. This system deals with the frequency selectivity of the channel by dividing the broadband data into parallel narrowband channels. Additionally, in a delay-dispersive environment, adopting a CP of a length greater than the maximum delay spread provides an excellent way to assure the orthogonality of the carriers. However, propagation is considered to be time selective due to the Doppler shift in which one subcarrier may introduce ICI to the adjacent subcarriers [1]. The Doppler shift sensitivity is inversely proportional to the OFDM symbol duration; therefore, even slightly moving platforms can cause serious impairments as far as synchronization is concerned.

Previous studies in the field of UWAC have addressed several approaches for synchronization in the presence of Doppler distortion. For single carrier transmission, a block-based approach [2] has been used to estimate and compensate the Doppler shift. In this approach, two LFMs are used for a coarse estimation of the time scaling factor and then an equalizer is employed for residual Doppler-shift compensation. This method is particularly well suited for constant speed. An alternative approach utilizes an adaptive Doppler compensation technique, as suggested by [3], in order to accommodate autonomous vehicles (AV). This closed-loop Doppler correction method demands a high degree of complexity when it is applied to OFDM systems because there is a requirement for the demodulation of each interpolation factor.

As far as multicarrier transmission is concerned, the authors in [4] employed the principle in [2] and null subcarriers for the purpose of resampling factor estimation and residual Doppler compensation, respectively. Although these algorithms do attain precise estimation by adopting preamble and postamble, the bandwidth utilization factor is compromised. A point estimate of the Doppler shift is adopted in [5]; therefore, it is suitable for situations where the Doppler shift stays constant or varies slowly during the packet time. The concept in [6] was extended to work in UWAC by [7] with an iterative cyclic prefix correlation. To estimate the Doppler shift, the author employed the symmetry of the guard interval with its replica. This parameter is estimated iteratively, depending on the peak location and its phase with respect to the new sampling interval; therefore it is a computationally expensive search. In [8], the authors deal with the different Doppler distortion in the multiple-input multiple-output (MIMO) OFDM by adopting multiple resampling followed by FFT.

Although resampling the signal removes the Doppler shift, a major problem with its residual or carrier frequency offset (CFO) is the destruction of the orthogonality of the subcarriers due to the resulting ICI. A considerable amount of literature on combating ICI has been published. These studies [1, 9–11] have presented conclusions that mitigating ICI will result in successful communication.

All the aforementioned papers assume that the Doppler shift is constant during the symbol period and all paths have equal Doppler shift; therefore, resampling the signal with a unique time scaling factor is valid and a symbol by symbol approach works effectively. A recent study by [12] has highlighted the need to estimate the optimal time scaling factor in a multipath channel of different Doppler shift in each path. However, in our proposed method, it is assumed that the channel variation is mainly caused by the motion of both transmitter and receiver, leading to a significant time-varying Doppler shift. Consequently, this will create acceleration that may exceed $1\,\mathrm{m/s^2}$ due to speed alterations; therefore, ignoring this effect yields a significant ICI. In this paper, the acceleration is considered and the Doppler shift is assumed to be changing linearly during the symbol time, but the same for all paths. This variation is dealt with by measuring the time expansion/compression frequently within a fraction of a sample period and then compensating the Doppler by means of an efficient 4th order Lagrange interpolation.

In this paper, an algorithm which combines the centroid-based localization and linear equation in estimating the time-varying Doppler shift is proposed. Furthermore, this paper introduces two improvements in order to increase the confidence of the Doppler shift estimation and consequently a low bit error rate (BER) is obtained. These improvements include:

(1) fine tune the coarse timing estimation; then,

(2) combining two correlation lags and fine tuning using the weighting coefficients [13]. The first lag is estimated based on the centroid localization [14], and the second lag is estimated based on the correlation of the cyclic prefix (CP) with its replica.

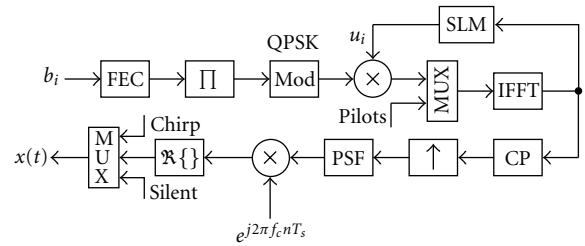

Figure 1: Proposed transmitter structure, where the operator $\Re$ represents the real part of the signal.

Additionally, for the case of low acceleration, these improvements result in a precise estimation of the Doppler shift and no CFO estimation is required.

The rest of this paper is organized as follows. In Section 2, the OFDM system model is introduced. The signal processing in the proposed receiver is presented in Section 3. In Section 4, Doppler extraction and channel estimation are demonstrated. In Section 5, the performance of the proposed algorithms are presented by means of experimental results. Finally, Section 6 draws the conclusions.

2. System and Channel Model

The proposed system contains the transmitter depicted in Figure 1. At each instant i, the encoder receives a vector of information bits b_i of length K_d at its input to produce a binary code of length $K_c = K_d/R_c$ encoded bits, where $R_c \in (0, 1]$ is the coding rate of the nonsystematic convolutional (NSC) code. The coded bits are permuted by a random interleaver, then converted, in groups of m successive bits, into alphabet symbols of constellation size $M = 2^m$. This mapping operation generates a sequence of $N_d = K_c/m$: $\mathbf{s} = \{s_0, \ldots, s_{N_d-1}\}$, where $s_i \in \mathbb{C}$ and $\mathbb{C}$ denotes the set of complex symbols. Subsequently, in the OFDM symbol to be constructed, pilot symbols of phase shift keying (PSK) with unit amplitude are embedded with the data symbols in a comb method, where all pilots and data are transmitted simultaneously on all symbols. These pilot symbols are used for the purpose of estimating channel response at the receiver. A peak-to-average power reduction (PAPR) is introduced using the selective mapping (SLM) technique [15]. To implement this technique, a sequence of phases $\mathbf{U}$ is added in the transmitted signal to be multiplied by the input data sequences, and the symbol sequence of minimum PAPR is selected for transmission. The resulting OFDM symbol, containing N_p pilots and N_d data-bearing subcarriers, where $N_d \cup N_p = N_c$, is then modulated by an IFFT of size N_c, and the last samples are copied and prefaced to the symbol to form the CP-OFDM frame. The guard interval of length N_g is chosen to be longer than the channel dispersion time in order to minimize the intersymbol interference (ISI). The resulting frame is pulse shaped, using a pulse shape filter (PSF), and then up converted using carrier modulation. Let T_d denote the OFDM symbol duration and T_g the guard interval. The total OFDM frame duration is $T = T_d + T_g$. Let $f_n = f_c + n\delta f$, being the carrier frequency corresponding to each of the subcarriers of the OFDM spectrum, where $\delta f = 1/T_d$ is

the frequency separation between alternate subcarriers, and f_c is the carrier frequency, so the bandwidth is $B = N_c\delta f$. The time-domain representation of the ith OFDM symbol is given by

$$x_i(t) = \frac{1}{\sqrt{N_c}} \sum_{n\in\mathcal{I}} d_i(n) u_i^{\text{opt}}(n) e^{j2\pi(n/T_d)(t-T_g-iT)} p_{\text{rc}}(t-iT), \quad \text{for } iT \le t < (i+1)T, \tag{1}$$

where $d_i(n)$ is the symbol transmitted over the nth subcarrier, $\mathbf{U}^{\text{opt}}$ is the optimum phase set $[u_i(1), u_i(2), \ldots, u_i(n)]$ for lower PAPR with $u_i(n) = e^{j\varphi_n}$, $\varphi_n \in [0, 2\pi]$, $\mathcal{I}$ denotes the set of modulated subcarriers, and $p_{\text{rc}}(t-iT)$ is the pulse shaping filter, which is realized as an up-sampled raised cosine FIR filter. An equivalent passband model of (1) is

$$\begin{aligned} x(t) &= \Re\left\{ e^{j2\pi f_c t} \sum_{i=0}^{\infty} \frac{1}{\sqrt{N_c}} \times \sum_{n\in\mathcal{I}} d_i(n) u_i^{\text{opt}}(n) e^{j2\pi(n/T_d)(t-T_g-iT)} p_{\text{rc}}(t-iT) \right\} \\ &= \Re\left\{ \sum_{i=0}^{\infty} \frac{1}{\sqrt{N_c}} \times \sum_{n\in\mathcal{I}} d_i(n) u_i^{opt}(n) e^{j2\pi f_n(t-T_g-iT)} p_{\text{rc}}(t-iT) \right\}. \end{aligned} \tag{2}$$

It is assumed that the signal is transmitted over a multipath fading channel as follows:

$$h(\tau, t) = \sum_{l=0}^{L-1} h_l(t)\delta[\tau - \tau_l(t)], \tag{3}$$

where $\{h_l(t)\}$ are the path amplitudes, $\{\tau_l(t)\}$ are the time-varying path delays, and L is the total number of paths. As in [16], we assume the path delay τ_l and the gains h_l are constant over the frame duration T. For perfect OFDM synchronization, and providing that the maximum delay spread is within the guard interval, the received passband signal can be written as

$$\tilde{r}(t) = \Re\left\{ \frac{1}{\sqrt{N_c}} \sum_{n\in\mathcal{I}} d_i(n) u_i^{\text{opt}}(n) e^{j2\pi f_n t} \times \sum_{l=0}^{L-1} h_l p_{\text{rc}}(t-\tau_l) e^{-j2\pi f_n \tau_l} \right\} + \tilde{w}_i(t), \tag{4}$$

where $w_i(t)$ is a white Gaussian noise with variance σ^2.

When the Doppler shift is present, a transmitted signal is received as

$$r(t) = x\left[\left(1 \pm \frac{v}{c}\right)t - \tau_l\right], \tag{5}$$

where v denotes the induced speed due to the mobility of the transmitter and/or receiver, and c is the acoustic propagation speed of 1500 m/s. The (+) sign indicates an expansion of the signal since the distance is increased and vice versa. It is assumed that all paths have a similar Δ; therefore, the received signal in (4) can be rewritten as

$$\tilde{r}(t) = \Re\left\{ \frac{1}{\sqrt{N_c}} \sum_{n\in\mathcal{I}} d_i(n) u_i^{\text{opt}}(n) e^{j2\pi f_n(1+\Delta)t} \cdot \sum_{l=0}^{L-1} h_l p_{\text{rc}}((1+\Delta)t - \tau_l) e^{-j2\pi f_n \tau_l} \right\} + \tilde{w}_i(t). \tag{6}$$

Based on the assumption that the speed of the motion changes linearly during the ith OFDM symbol interval $t \in [iT, T(i+1))$, the Doppler shift is varied with time. Therefore the constant $\Delta = v/c$ does not hold to accommodate this variation and it should be replaced by $\Delta(t)$. Thus, the time varying Doppler shift can be modelled as

$$\Delta(t) = \frac{v(t)}{c}, \tag{7}$$

where $v(t)$ represents the speed variation during the symbol time. Therefore, the received passband signal in (6) can be rewritten as

$$\tilde{r}(t) = \Re\left\{ \frac{1}{\sqrt{N_c}} \sum_{n\in\mathcal{I}} d_i(n) u_i^{\text{opt}}(n) e^{j2\pi f_n(1+\Delta(t))t} \cdot \sum_{l=0}^{L-1} h_l p_{\text{rc}}[(1+\Delta(t))t - \tau_l] e^{-j2\pi f_n \tau_l} \right\} + \tilde{w}_i(t), \tag{8}$$

and its corresponding complex baseband signal model can be written as

$$r(t) = \sum_{i=0}^{\infty} \sum_{n\in\mathcal{I}} H_i(n) d_i(n) u_i^{\text{opt}}(n) e^{j2\pi n\delta f t} e^{j2\pi\Delta(t) f_n t} + w_i(t), \tag{9}$$

where $H_i(n)$ is the channel transfer function of the ith symbol at nth subcarrier with a time varying Doppler-shift that can be written as

$$H_i(n) = \sum_{l=0}^{L-1} h_l e^{-j2\pi f_n \tau_l} p_{\text{rc}}[1 + \Delta(t)t - \tau_l]. \tag{10}$$

As referred to in [17], it is obvious in (9) that the effect of the Doppler shift on the received signal is twofold. Firstly, it scales the received OFDM frame duration T by a factor of $1 + \Delta(t)$, yielding sampling frequency errors that result in a symbol timing error [18]. Secondly, there is a time-varying CFO.

2.1. Sampling Frequency Errors. In discrete time, the sampled transmitted signal $x[kT_s]$ in (5) is equivalent to a scaling of the sampling period (interpolation or decimation).

$$\tilde{r}[kT_s] = x[k(1 \mp \Delta(t))T_s - \tau_l], \tag{11}$$

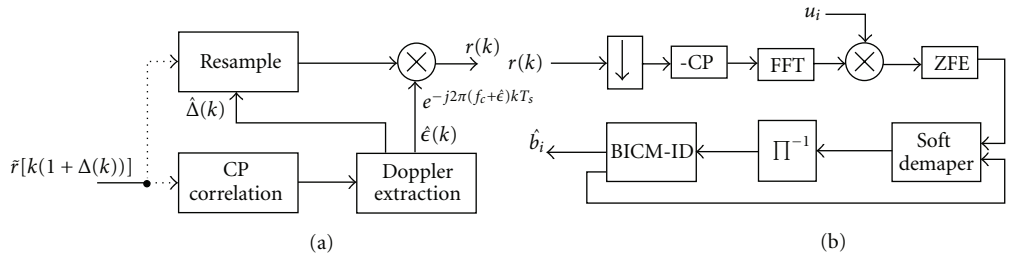

Figure 2: Proposed receiver structure.

where k is an integer, and T_s and $\tilde{r}(kT_s)$ are the sampling period and Doppler shifted received sampled signals respectively.

The bidirectional effect of the Doppler shift causes symbol timing errors, which are increased or decreased proportionally to $\Delta(t)$. To align the symbol within its period, samples should be removed if $(\Delta > 0)$ or added if $(\Delta < 0)$ at regular intervals [19].

Let $\pm\phi$ be the deviation of samples of the received sequence for each OFDM symbol due to the speed change; the sampling period results in expansion or compression of the samples' length, hence the Doppler-shifted received frame's length is modelled by

$$L'_f = \left(L_f \mp \phi\right), \tag{12}$$

where $L_f = (N_c/B \cdot T_s)$ represents the transmitted passband samples' length. It is apparent that L_f is only affected by T_s and any expansion/compression in the timescale will result in ϕ. Therefore, (12) is implicitly equivalent to (11). To remove both CFO and symbol shift, an inverse time scaling of the received (compressed/expanded) signal should be achieved, providing that the amount of Doppler shift $\Delta(t)$ is known. This is equivalent to changing the sampling rate of the passband signal by $1+\Delta(t)$ in discrete-time processing. From (12), it can be inferred that increasing or decreasing the length of samples is equivalent to adjusting the sampling frequency f_s by the same Doppler shift $1 + \Delta(t)$; thus, (11) is rewritten as

$$\tilde{r}[k] = x\left[\frac{k(1 \mp \Delta(t))}{f'_s} - \tau_l\right], \tag{13}$$

where $f'_s = f_s(1 \mp \Delta(t))$. By substituting f'_s in (13), $\tilde{r}[k] = x[k]$, the signal received is then in conformity with the transmitted signal.

2.2. Carrier Frequency Offset Errors. The factor $e^{j2\pi\Delta(t)f_n t}$ in the received signal in (9) represents a time varying CFO, where $\Delta(t)f_n = \Delta(t)f_c + \Delta(t)n\delta f$. The CFO (ϵ) is due to the residual Doppler shift. It is destructive because it deviates the subcarrier spacing δf and introduces ICI, which must be removed prior to the FFT to design an optimum receiver [18]. The resampling process removes the Doppler shift and converts the wideband system into narrowband. However, the residual Doppler shift produced by the fractional part of the time expansion/compression degrades the receiver.

3. Signal Processing in the Proposed Receiver

To utilize the available bandwidth efficiently, the algorithm employs a low-complexity blind technique to estimate the Doppler shift based on estimating the coarse timing metric for each OFDM symbol by exploiting the inherent periodicity of the CP. Centroid-based localization has been used to refine the maximum amplitude of the timing metric, that is, the timing offset, as explained in [14]. Using this coarse timing metric, the Doppler shift and its residual are frequently estimated by deriving a tracking step in the Doppler extraction unit (DEU). This unit comprises linear expectation of the timing offset, fine tuning of the estimated parameters, tracking the Doppler shift, and CFO estimation. In this technique, the fractional deviation of the subcarrier spacing, which is the source of ICI, is estimated by exploiting the fractional part of the normalized sampling frequency offset, whereas the integer part of this offset is used to estimate the integer Doppler shift.

3.1. Coarse Timing Metric Estimation. The receiver structure of the proposed system is depicted in Figure 2. The received signal $\tilde{r}(t)$ in (8) is fed through the transducer, preamplifier, and analogue-to-digital converter, and then filtered in the frequency band $[f_c - B/2, f_c + B/2]$. The resultant Doppler shifted passband signal $\tilde{r}[k(1 + \Delta(k))]$ is correlated with the Doppler tolerant training (chirp) to detect the start of the packet ζ that contains several OFDM symbols. Based on the existing guard interval, the drift in the received Doppler-shifted signal $\tilde{r}[k(1 + \Delta(k))]$ is measured by correlating the guard samples $(N_g \cdot N_s)$ with an anticipated observation window in order to estimate the coarse timing metric for each OFDM symbol within the packet, as in [14]. In the case of time-varying Doppler shift, that is, multi time scaling factor, the resulting timing metric is affected by the velocity perturbation. Consequently, there is a demand on estimating this timing metric of the same OFDM symbol, but using an alternative approach to increase the accuracy of the Doppler shift estimation. Therefore, in Figure 2(a), linear prediction is adopted to extract the Doppler shift for the purpose of reinforcing the symbol timing offset parameter that was estimated using CP correlation.

3.2. Time-Varying Doppler Shift Estimation. Thus far, the timing metric has only been considered for the case of a common Doppler shift during the OFDM symbol time. A worst case scenario may occur when there is a velocity that

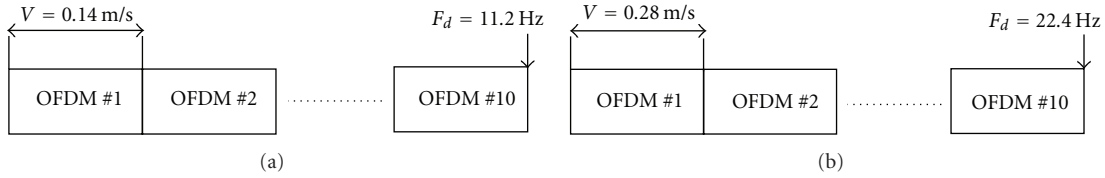

Figure 3: Acceleration effect over Doppler frequency change during each symbol time at $f_c = 12$ kHz. (a) Acc = 0.5 m/s^2, (b) Acc = 1 m /s^2.

accelerates or decelerates within the symbol period. This situation can be explained in Figure 3. This figure shows that the start of the OFDM symbol undergoes a different speed relative to the speed at the end of the symbol due to the acceleration, in which the speed is changing linearly with time. As a result, a linear multi Doppler shift during the OFDM symbol period is produced. In addition, the acceleration is a useful indication of how fast the change is, where in Figure 3(a) the Doppler frequency shift is 1.12 Hz at OFDM symbol 1 and it increases to 11.2 at OFDM symbol 10. The same case is demonstrated in Figure 3(b), where the acceleration is 1 m/s^2 and the Doppler frequency at OFDM symbol 10 is 22.4 Hz, in terms of time-selectivity measurement which is given as

$$T_d F_d > 1. \tag{14}$$

This rapid change within the symbol duration gives an indicator of the amount of distortion caused by the channel on the signal.

Alternatively, frequent estimation of the Doppler shift within the OFDM symbol or reducing the frame length are viable solutions. However, in OFDM signal design, there is a tradeoff between the number of subcarriers, Doppler estimation resolution, and sensitivity to the CFO. Hence, frequent estimation of the interpolation factor is more feasible than shortening the OFDM symbol length.

When the channel has a velocity that accelerates or decelerates in both directions (up or down) within the symbol period, the following example is considered. If T_d is 256 ms and the maximum acceleration 1 m/s^2 starting from initial speed v_0, then the symbol needs approximately $4T_d$ to attain the maximum speed $v_0 + 1$ m/s. From this assumption, it can be inferred that the maximum speed change in each OFDM symbol is approximately 0.25 m/s.

For a system of 12 kHz carrier frequency, 48 kHz sampling frequency, and a symbol time of 0.256 seconds, such speed variation causes a Doppler frequency shift F_d to increase by 2 Hz within each symbol up to 20 Hz by symbol number 10. In such circumstances, estimating a common timing metric may not hold to attain acceptable performance. Alternatively, a better solution and more accurate Doppler compensation can be realized by adopting a frequent estimation of the Doppler shift within the OFDM symbol.

4. Doppler Extraction and Channel Estimation

The Doppler extraction unit in Figure 2(a) comprises linear prediction of the symbol timing offset, fine symbol timing offset, tracking the Doppler shift and CFO or residual Doppler shift estimation.

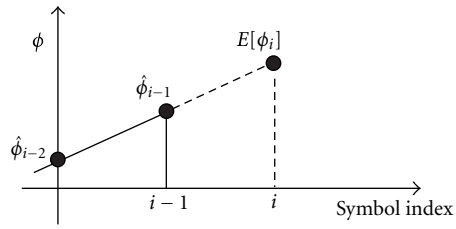

Figure 4: Estimation of timing offset during the packet time.

4.1. Linear Prediction of the Symbol Timing Offset. As the transmission structure contains multiple OFDM frames within a packet, the synchronization between these frames is paramount to reduce both the ISI and ICI on the receiver side. In the proposed technique, an improvement is obtained by involving the estimated timing offset at time $i-1$ in predicting the timing offset at time i. To accomplish this, it is assumed that due to the first order Doppler shift, the OFDM frame could be expanded towards the leading edge or compressed towards the trailing edge in the range $[T(1+\Delta(t))+\tau_{\max}, T(1-\Delta(t))+\tau_{\max}]$, respectively. Therefore, the linear part of the speed variation can be formulated by the following first order equation:

$$y = mx_i + b, \tag{15}$$

where $m = (\hat{\phi}_i - \hat{\phi}_{i-1})/(x_i - x_{i-1})$ denotes the slope, and x_i is the OFDM symbol at index i, as shown in Figure 4. Accordingly, the gradient will vary gradually in accordance with the speed change and, subsequently, the output value y_i is obtained. The slope here is determined based on the previous two OFDM symbols estimated in (17) and subsequently used to predict the timing offset ϕ for the next OFDM symbol. Therefore, the first order predicted timing offset of the current OFDM symbol can be formulated as

$$E[\phi_i] = 2\hat{\phi}_{i-1} - \hat{\phi}_{i-2}. \tag{16}$$

4.2. Fine Symbol Timing Offset and Synchronization. Thus far, two estimations of the same parameter $\hat{\phi}$ have been obtained. It should be stressed that attaining accurate timing offset estimation may be difficult in the presence of noise and/or ISI, especially with a short observation window. Therefore, for the purpose of increasing the reliability of

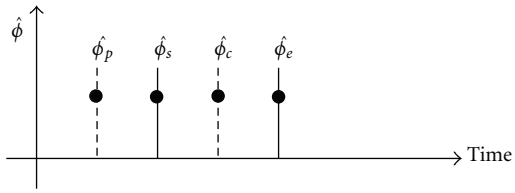

Figure 5: Tracking the Doppler within the OFDM symbol.

estimation, smoothing the timing offset is adopted. This yields the following fine tuned estimated timing offset:

$$\hat{\phi}_i = \hat{\phi}_i W_1 + E[\phi_i] W_2, \tag{17}$$

where the coefficients W_1 and W_2 are empirically obtained and satisfy the condition of $0 < W_1 + W_2 \leq 1$. These coefficients are designed to attain a tradeoff between estimation accuracy and tracking capabilities. It is crucial to mention that these coefficients have an effect on adapting the slope variation, where $W_1 = 1, W_2 = 0$ indicates fast slop variation and the linear expectation does not hold. At the same time, $W_1 = 0, W_2 = 1$ accommodate a constant gradient between symbols. The estimated fine timing offset $\hat{\phi}$ in (17) still represents the average. Assuming the change in the time scale is linear within the OFDM symbol, the change in the speed is considered unidirectional. This will enable tracking of the Doppler shift caused by speed variation within the OFDM symbol time. Performing such tracking demands knowledge of the timing offset at both edges of the symbol in order to determine the tracking step. By involving previous estimation of fine symbol timing offset $\hat{\phi}_p$ and current fine symbol timing offset $\hat{\phi}_c$, the offset at the leading edge can be formulated as

$$\hat{\phi}_s = \frac{\phi_p + \phi_c}{2}. \tag{18}$$

At the same time, the sampling frequency offset at the trailing edge $\hat{\phi}_e$ is determined as

$$\hat{\phi}_e = 2\hat{\phi}_c - \hat{\phi}_s, \tag{19}$$

where $\hat{\phi}_p$ and $\hat{\phi}_c$ represent the average fine timing offset estimate from (17). It should be stressed that the estimation accuracy of these two parameters plays an important role in increasing the ability to compensate for the Doppler shift and its residual effects in the subsequent stages.

4.3. Tracking the Doppler Shift. If the relative velocity between the transmitter and receiver during the packet time is constant, that is, for zero acceleration, then the Doppler shift estimate computed can be used to compensate for the entire OFDM symbol. In time varying Doppler shift, however, a unique interpolation factor for the whole symbol does not hold due to the resulting nonnegligible sampling frequency errors which must be tracked. Therefore, the sampling frequency offset affects channel estimation, which is computed over pilot subcarriers, due to the different delays of the positions of these pilots. By searching for the delay in the 1st significant arrival of the estimated CIR [20], an approach to tracking the fractional sampling clock frequency offset due to a symbol timing error is possible. However, in the case of time-varying Doppler shift, it is necessary to estimate the sampling frequency offset frequently.

An alternative realistic Doppler shift estimator, which can be realized by adopting frequent estimation of this parameter during the symbol time in the time domain, is proposed here. In order to track the Doppler shift, it is necessary to derive a tracking step that corresponds to the sampling frequency offset change over $\hat{\phi}_s < \hat{\phi}_s + T_s < \hat{\phi}_e$. In such a case, the tracking step is given as

$$\phi_{\text{step}} = \frac{\hat{\phi}_e - \hat{\phi}_s}{L_f}, \tag{20}$$

where L_f represents the up-sampled subcarriers. As shown in Figure 5, each OFDM symbol is identified by the two parameters of sampling frequency offset $\hat{\phi}_s$ and $\hat{\phi}_e$, based on the assumption that the speed changes linearly. Accordingly, the estimated timing offset at the leading edge is updated at each sample time k, based on the step in (20). At the same time, the integer Doppler shift can be computed as

$$\hat{\Delta}(k) = \frac{L_f - \hat{\Psi}(k)_{(\text{quant})}}{L_f}, \tag{21}$$

where Ψ is the sampling frequency offset initialized with $\hat{\phi}_s$, and then updated at each sample as

$$\Psi(k) = \Psi(k-1) + \hat{\phi}_{\text{step}}, \tag{22}$$

and $\hat{\Psi}_{(\text{quant})} = \lceil \hat{\Psi} \rfloor$ is rounded towards the nearest integer, respectively. This integer resampling factor is delivered to the sample-by-sample Lagrange quadratic interpolation unit, as shown in Figure 2(b), and the fractional part is dealt with as a carrier frequency offset. It should be stressed that the resolution of the interpolation factor in (21) is entirely dependent on the transmitted frame length.

4.4. Residual Doppler Shift Estimation. Efficient Doppler shift compensation relies on how accurately the resampling factor estimation reduces the residual Doppler. This residual Doppler has a direct impact on the performance of the receiver. Taking this effect into account involves finding the amount of the fractional part of the estimated samples that shifts the subcarrier spacing fractionally. This deviation can be modelled as $(\hat{\Psi}(k) - \hat{\Psi}_{(\text{quant})})$, and therefore

$$\hat{\epsilon}(k) = \left[\hat{\Psi}(k) - \hat{\Psi}_{(\text{quant})}\right] \delta f \frac{f_c}{f_s}, \tag{23}$$

is the residual frequency estimate. The residual Doppler shift is not constant at each sample within the OFDM symbol, and thus it is dealt with by determining the standard deviation across the fractional part of the estimated Doppler shift. Once the Doppler shift and its residual have been estimated

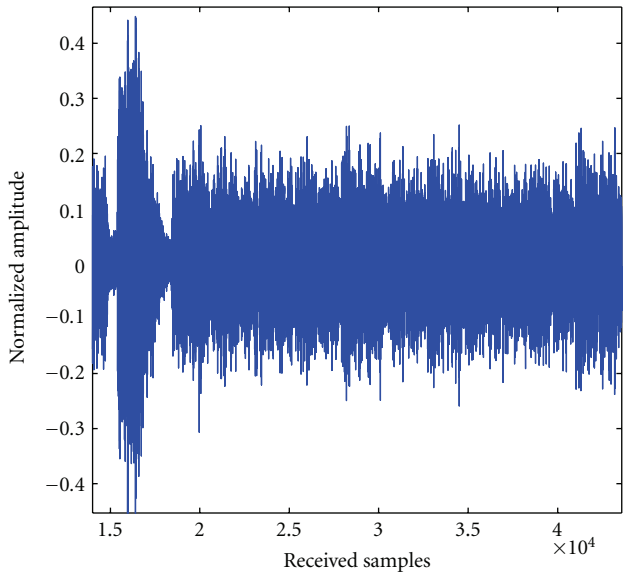

Figure 6: Received signal.

and compensated, the output signal $r(k)$ is delivered to the outer receiver in Figure 2(b). This signal is firstly down sampled and then its cyclic prefix is discarded. The PAPR phases $\mathbf{u_i}$ are removed prior to FFT demodulation. The zero forcing equalizer (ZFE) and least square (LS) method for channel estimation purposes are adopted by utilizing pilots which are embedded in a comb method. After removing the channel effect, the subsequent stage is BICM-ID.

4.5. Pilot-Based Channel Estimation. In the channel estimation of the OFDM symbol, a comb-type arrangement of the training sequence (pilot) is adopted. In this scheme, specific tone indices are allocated on all transmitted OFDM symbols and the rest for data transmission. Unlike a block-based training sequence, the comb type is quite convenient for fast fading channels. Additionally, with the comb type, all pilots and data are transmitted simultaneously on all symbols.

It is worth pointing out that in order to increase the accuracy of the channel estimation, the residual Doppler shift should be eliminated [21]. This is due to an induced ICI which destroys the orthogonality among subcarrier frequency components and ultimately the diagonal of the channel matrix. In OFDM systems, the advantage of increasing the symbol duration in reducing the ISI effect can conflict with increasing the ICI impact, as a consequence of subcarrier spacing reduction. Therefore, after resampling and CFO compensation, all subcarriers are orthogonal (i.e., ICI free).

The channel estimation was implemented using the following least square (LS) method [22]:

$$X(n) = X(mL + l) = \begin{cases} X_p(m), & l = 0 \\ X_d(m), & l = 1, \ldots, L-1, \end{cases} \quad (24)$$

where $L = N_c/N_p$ and $X_p(n)$ is the nth pilot subcarrier value. Let $H_p(n)$ be the frequency response of the channel for $n = 0, \ldots, N_p - 1$ at pilot subcarriers. Let $Y_p(n)$ be the received pilot symbols after the FFT operation, the estimate of the channel at pilot subcarriers $\hat{H}_p(n)$ is given as

$$\hat{H}_p(n) = D\left[X_p(n)\right]^{-1} Y_p(n), \quad n = 0, \ldots, N_p - 1, \quad (25)$$

where $D[X_p(n)]$ is a diagonal matrix constructed using the known transmitted pilot symbols.

For subcarriers $n = 0, 1, 2, \ldots, N_c - 1$, LS channel estimation $\hat{\mathbf{H}}_{\mathrm{LS}}$ is written as

$$\hat{\mathbf{H}}_{\mathrm{LS}}[n] = \frac{\mathbf{Y}[\mathbf{n}]}{\mathbf{X}[\mathbf{n}]}. \quad (26)$$

The mean square error of the LS channel estimation is considered high when compared with the minimum mean-square error (MMSE) estimate [23]. However, LS is attractive in implementing real-time systems due to its simplicity. In order to increase the reliability of the channel estimation, an interpolation in frequency domain between each pilot and data subcarriers is adopted. It is well known that the LS is the first step of the channel frequency response estimation for the known pilots and should be followed by interpolation to obtain a nonpilot subcarriers frequency response.

5. Experimental Results

During the summer of 2009, an experiment was conducted in the North Sea to evaluate the system performance. In the trial setting, the transmitter and receiver were set at 10 and 5 m from the sea surface, respectively. The set-up ranges between the transmitter and the receiver were 200 m, 500 m, and 1000 m. The transmitter power was set to 180 dB re 1 μPa@1 m which is the equivalent of approximately 10 W. In the trial, transmission was organized in packets of equal duration, each containing one 50 ms LFM followed by a 12.5 ms silent period and then 10 CP-OFDM frames. A total of 8920 information bits were transmitted in each setting. A total of 20 packets of 2.795 s were sent. The carrier frequency was set to 12 kHz, whereas the sampling frequency was $4f_c$. 1024 subcarriers were employed and the system bandwidth was 4 kHz, which led to a subcarrier spacing of 3.90625 Hz. The guard interval was set at T_g =16 ms. Figures 6 and 7 show the channel measurements over a range of 1000 m. These figures show a received frame structure and the normalized CIR of a packet that exhibits maximum delay spread of the order of 6 ms, respectively. This multipath delay is equivalent to an ISI of 24 symbols for a system bandwidth of 4 kHz, and this delay spread is inversely proportional to the range. In addition to the silent period shown in Figure 6, the CP guard time also contributes towards reducing the ISI effect.

5.1. Proposed Receiver Performance. To evaluate the performance of the proposed system, the experimental results for both block-based and proposed techniques are depicted in Figure 8(a). The performances of both receivers are presented

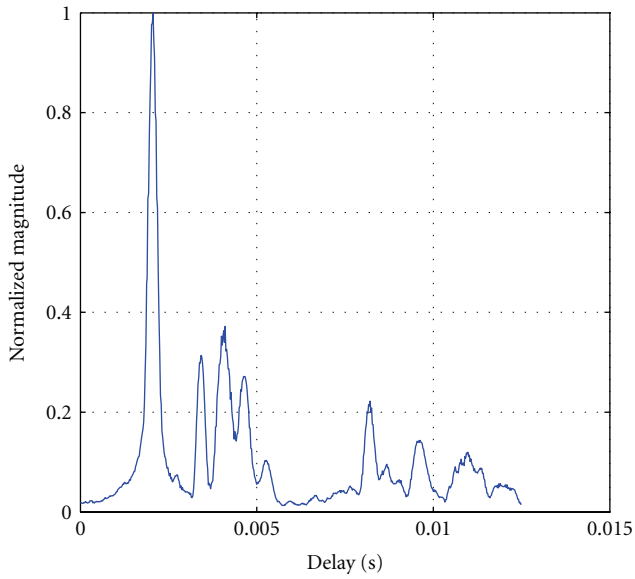

Figure 7: Sample of normalized channel impulse responses for 1000 m channel range.

Table 1: Average BER comparison of the experimental results at different settings of weighting coefficients between the proposed and block-based Doppler shift techniques for $N_c = 1024$.

Method	Error statistics	
	Errors	BER
Block	6503	0.0365
Proposed-set 1	772	0.004
Proposed-set 2	105	0.0006

Table 2: Performance of the experimental results between the improved and block-based Doppler shift techniques for $N_c = 1024$.

Packet index	1	2	3	4	5	6	7	8	9	10
Block	0	119	423	347	3	44	11	505	39	2443
Proposed	0	0	3	6	0	33	0	6	9	0
Improved	0	0	0	0	0	3	0	0	0	5
Packet index	11	12	13	14	15	16	17	18	1 9	20
Block	24	0	33	178	21	1702	21	0	471	119
Proposed	0	0	6	14	5	0	0	0	23	0
Improved	0	0	0	0	9	0	0	0	0	0

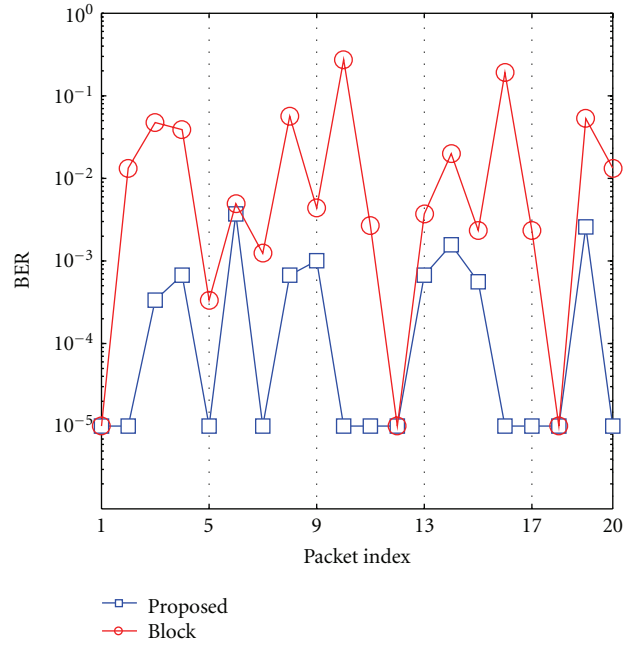

(a) BER for each packet over 1000 m range, where the label 10^{-5} represents zero error

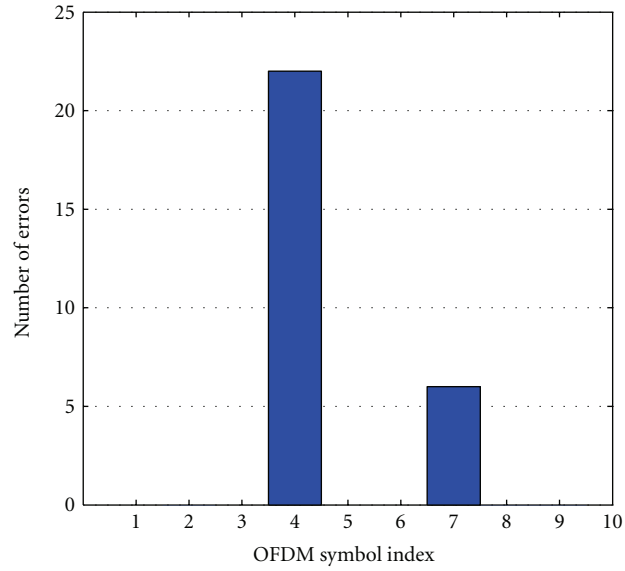

(b) Error statistics for packet 6; 2 out of 10 have decoding errors

Figure 8: Performance of the proposed system at 1024 subcarriers.

in terms of bit error rate (BER). In the block-based method, single resampling is performed for the received signal. It can be seen that for all packets the proposed technique outperforms the block-based method. This is further clarified in Table 2 which shows that the proposed technique achieves acceptable performance in reducing errors in all packets compared with the block technique. Error statistics for both schemes are presented in Table 1. It can be seen that compensating the time-varying Doppler scale and its residual leads to a reduction in the BER from 0.0365 to 0.0006, which is equivalent to 98.4%. However, Figure 8 shows high decoding error in packet 6.

In Figure 8, the bit errors are high only in two blocks within packet 6, as shown in Figure 8(b). This is due to the noise effect which affects the Doppler scale estimation when estimating the timing offset. Evidence for this is shown in Figures 9(b) and 9(d), where in packet 6 there is a mismatch in estimating the speed at the end of symbol 3 and at the start of symbol 4. Therefore, a decoding error results in symbol 4. Furthermore, it can be seen from Figure 9(a) that there is a relatively high deceleration of $\sim 0.9\,\text{m/s}^2$ during the symbol time, which adds an error in approximating the correlation-based Doppler scale estimation. This result shows that there

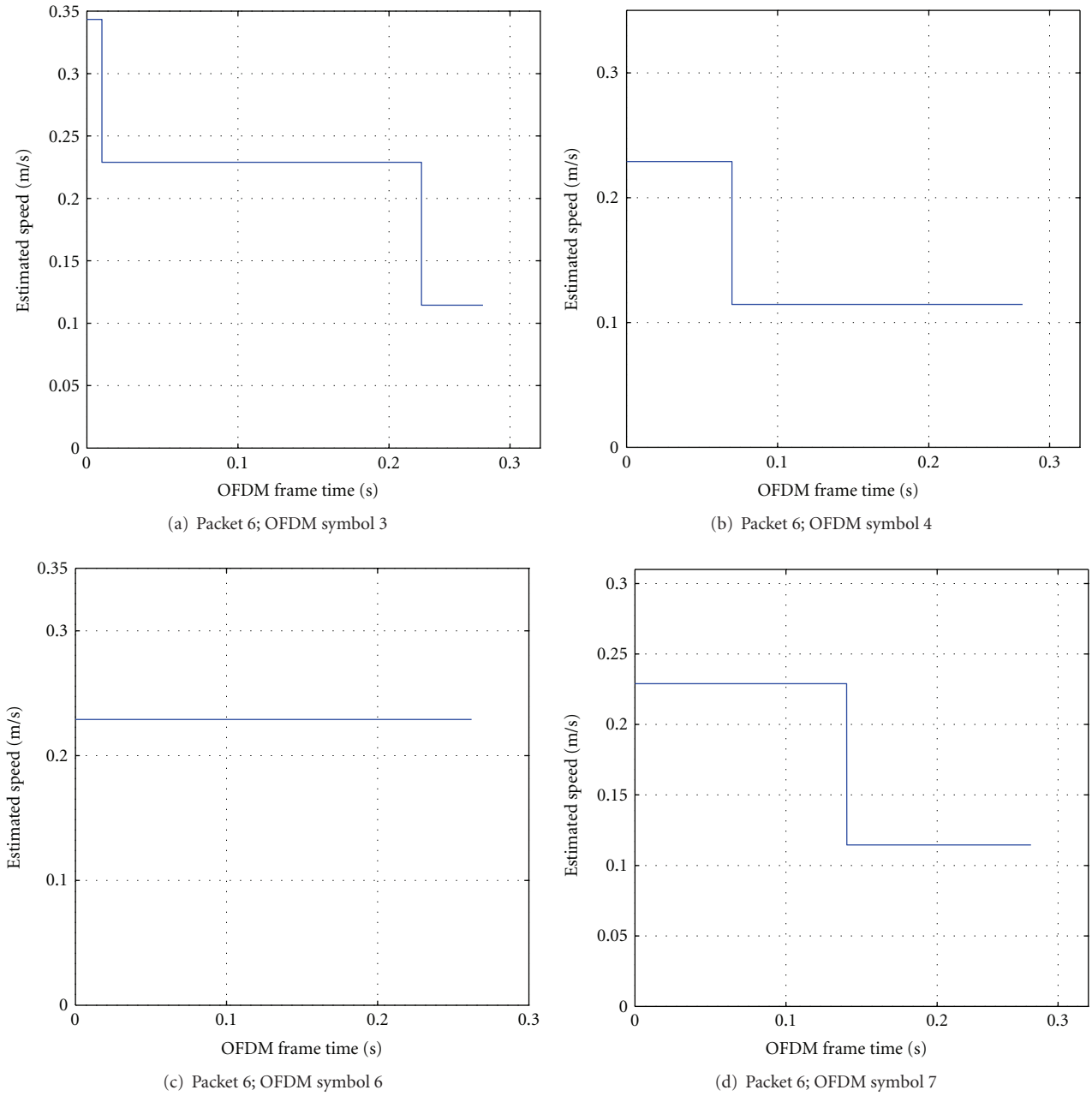

(a) Packet 6; OFDM symbol 3

(b) Packet 6; OFDM symbol 4

(c) Packet 6; OFDM symbol 6

(d) Packet 6; OFDM symbol 7

Figure 9: Estimated speed variation during OFDM symbol.

is a limitation on the acceleration that can be adopted in this algorithm.

Figure 9 demonstrates that the adopted system is capable of precisely tracking the speed variation in each symbol. Particularly, in Figure 9(a), the speed in symbol 3 of packet 6 has been changed three times during 0.256 s, whereas in Figure 9(c) the speed is constant. However, changing the direction of velocity within the packet period, along with higher acceleration, can produce higher intercarrier interference levels in the system. The source of this noise is the mismatch introduced by the transition from acceleration to deceleration, or vice versa. The proposed system detects this critical point through the CP correlation-based Doppler scale estimation, and the linear expectation has no effect on this scenario. However, linear expectation reduces the channel and/or noise effect on the CP correlation. Consequently, accurate Doppler scale estimation is obtained.

Figure 10 shows the performance of bit-interleaved coded modulation with iterative decoding (BICM-ID) and ZFE in the experiment. In terms of Figure 10(a), the figure shows that the ZFE delivers reliable information to the decoder. The reliability depends on how accurate the Doppler shift compensation is. It was mentioned earlier that the channel estimation is affected by the presence of residual Doppler shift which can cause ICI, and, as a result, the orthogonality is destroyed. Consequently, the iterative decoding stage can

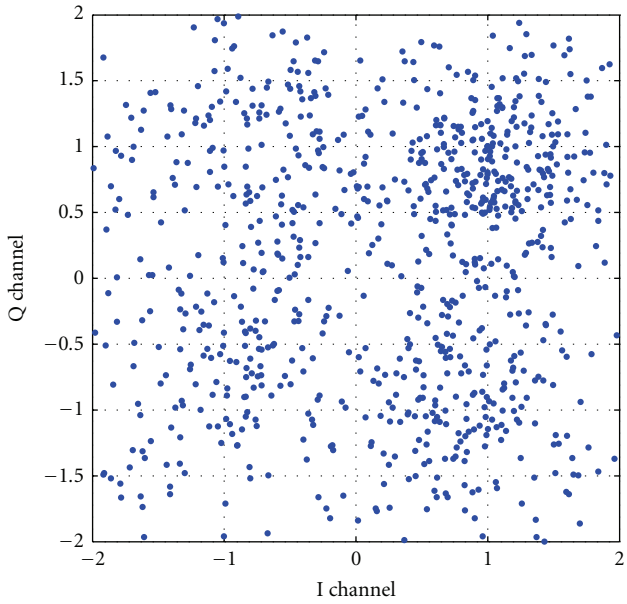

(a) I-Q Constellation at EQ-O/P

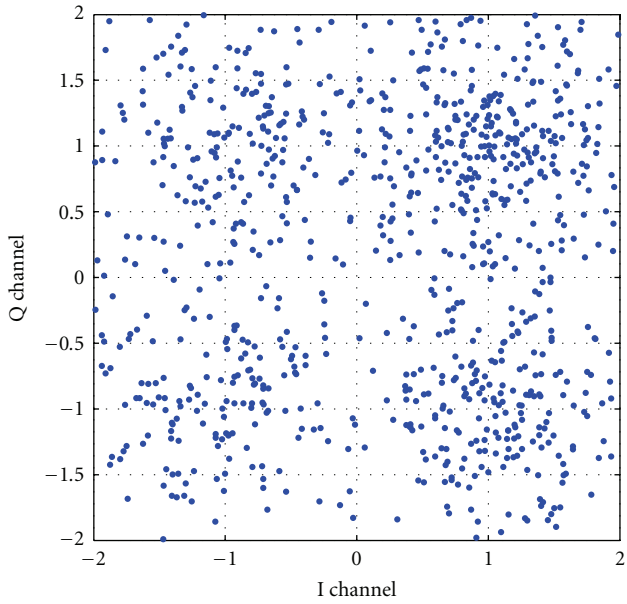

(b) I-Q Constellation at EQ-O/P: Iter-1

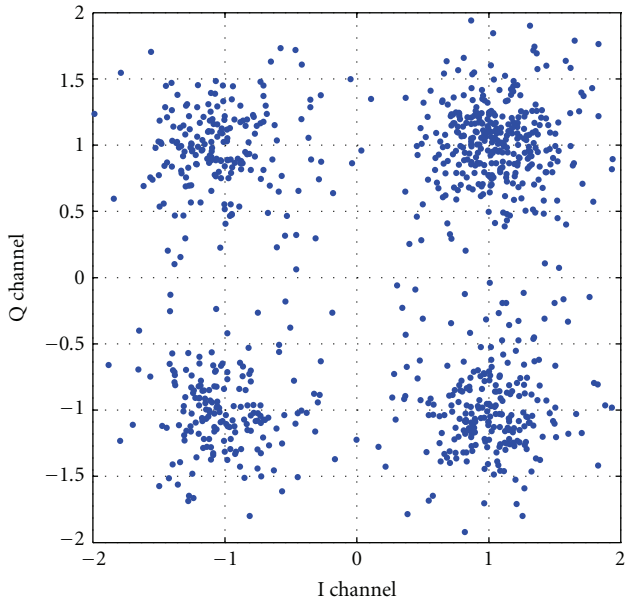

(c) I-Q Constellation at EQ-O/P: Iter-2

Figure 10: Constellation output from equalizer and iterative receiver.

generate unreliable LLRs [24]. Thus, it can be seen that there is an improvement in the second iteration in Figure 10(c) compared with the first iteration in Figure 10(b). At this stage, further iterations are pointless and no more gain is expected.

5.2. Effect of Weighting Coefficients. As mentioned in [13], the weighting coefficients play an important role in the accuracy of the Doppler scale estimation. For this reason, special settings of these parameters are required in order to achieve acceptable performance. It can be shown that there is a tradeoff between the value of the weighting coefficients and the receiver performance. To be more specific, by appointing the symbol timing offset, estimated by linear expectation, a lower weighting coefficient than correlation-based symbol timing offset estimation means there is a constant acceleration or deceleration between symbols, and vice versa. As shown in (17) and (20), the Doppler scale is approximated based on estimating the fine symbol timing offset and its tracking step is derived based on the sampling frequency offset at the start and end of the OFDM symbol. This means that the weighting coefficients have a direct effect on the estimation of the time varying Doppler scale $\Delta(t)$.

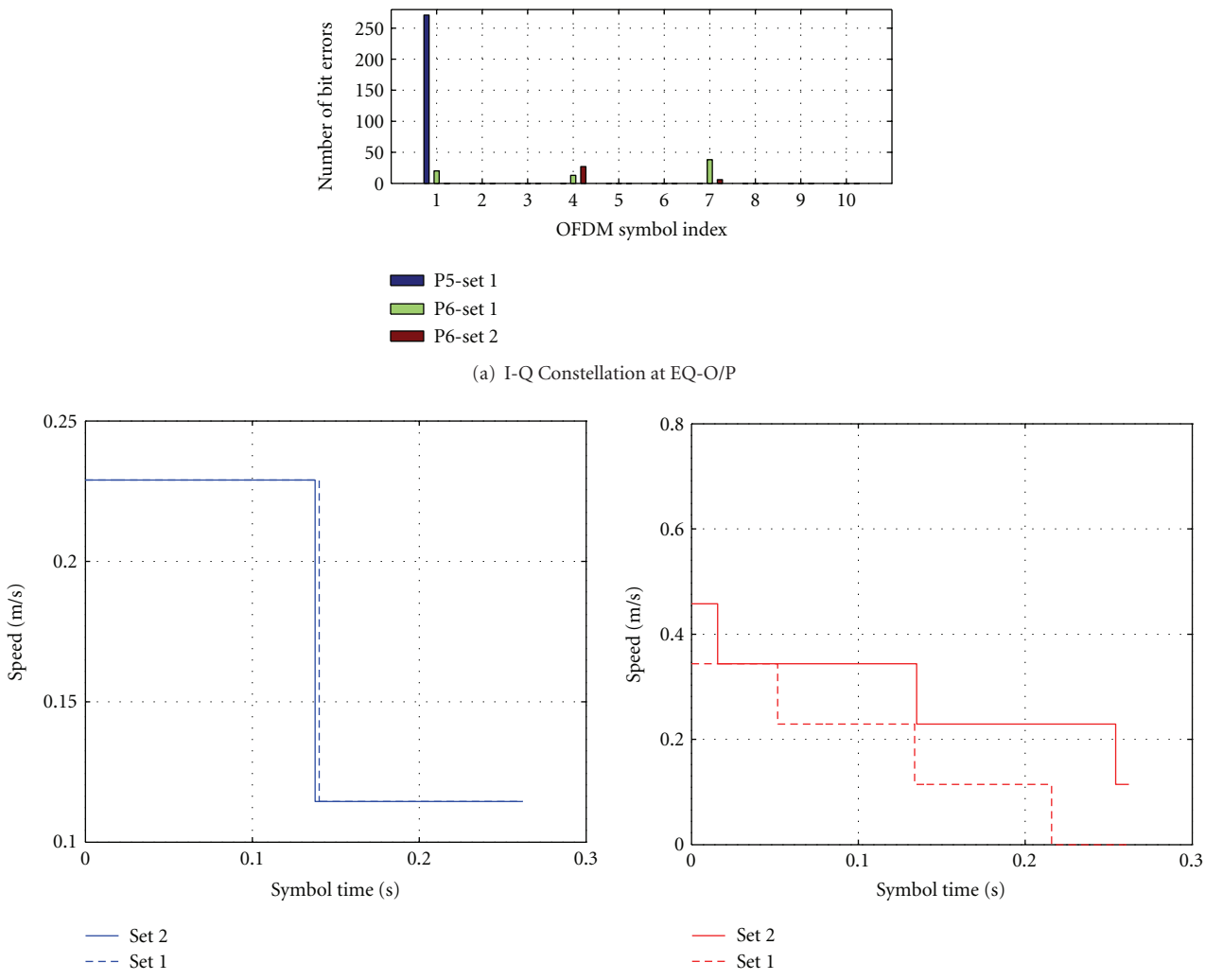

(a) I-Q Constellation at EQ-O/P

(b) I-Q Constellation at EQ-O/P: Iter-1

(c) I-Q Constellation at EQ-O/P: Iter-2

Figure 11: Effect of weighting coefficients on estimation.

Figure 11 shows two settings of these parameters and their effect on the performance of the receiver. In set 1, where $W_1 = 0.5$ and $W_2 = 0.5$, it can be seen that the receiver performance is poor. In Figure 11(a), it is obvious that packets 5 and 6 in set 1 exhibit a high BER of 271/8920 and 71/8920, receptively. The reason for this degradation is that increasing the weight of the linear expectation in a channel leads to significant acceleration that can cause maladjustment of the interpolation factor and make the tracking of the Doppler scale change coarsely. This is shown in Figure 11(c). Although both sets have the same slope, there is a mismatch between them at the start and end of speed estimation. In set 2, on the other hand, $W_1 = 0.85$ and $W_2 = 0.15$, there is a great improvement in the performance as shown in Figure 11(a), with 0 errors in packet 5 and 33 bits in packet 6. Table 1 shows the performance of the receiver for the subcarriers 1024 over a range of 1000 m using two different settings of the weighting coefficients. In set 2, it can be observed that the error decreases by about 86.4% compared with set 1.

5.3. Performance Evaluation with Improved Coarse Timing Estimation. As mentioned earlier, the impairments in the channel estimation due to synchronization failure will result in unreliable LLRs as a consequence of the Doppler effect. In contrast, estimating and compensating the Doppler scale precisely causes the received OFDM symbol to coincide with its transmitted period, thus improving the channel estimation and delivering reliable symbols to the decoder. Therefore, the target is to improve the Doppler scale estimation and ultimately reduce the burden on the channel estimation.

In order to extract the Doppler scale successfully, it is important to increase the reliability of estimating the symbol timing.

Considering the effect of acceleration on the chirp correlation is small, in the case of multiple OFDM symbols within a packet, the symbol timing error in each OFDM block is accumulated with acceleration during the packet time. Hence, adopting a single estimation of ζ for the whole packet is no longer accurate. Therefore, in order to mitigate the acceleration effect on the symbol timing error, ζ needs

to be fine tuned. Performing the fine tuning necessitates updating the position of ζ after each symbol time. Let m, i denote the range of the timing offset around the leading and the trailing edge during the OFDM symbol, respectively. It follows that a two-dimensional timing function is written as

$$\Lambda(m,i) \triangleq \left| \sum_{n=0}^{N_g-1} r(\zeta+m+n) r(\zeta+n+N+i) \right| \quad m \in \left\{-\frac{W}{2},\ldots,\frac{W}{2}\right\};\ i \in \left\{-\frac{\Upsilon'}{2},\ldots,\frac{\Upsilon'}{2}\right\}. \tag{27}$$

Then, $\hat{\theta}_{m,i}$ can be estimated from obtaining the maximum peak of the multiplication, and it can be written as

$$\hat{\theta}_{m,i} = \arg\max \max_{m,i} \Lambda(m,i) \quad m \in \left\{-\frac{W}{2},\ldots,\frac{W}{2}\right\};\ i \in \left\{-\frac{\Upsilon'}{2},\ldots,\frac{\Upsilon'}{2}\right\}, \tag{28}$$

and the fine tuned ζ' is obtained. The implementation of this fine tuning algorithm of the coarse packet synchronization can be summarized as follows:

(1) compute the coarse packet synchronization point ζ which represents the time position of the maximum peak of the chirp correlation,

(2) compute the timing function $\Lambda(m,i)$ for $m \in [-W/2, W/2], i \in [-\Upsilon'/2, \Upsilon'/2]$,

(3) choose the maximum of the maximum of $\Lambda(m,i)$ as the estimated packet timing offset,

(4) update ζ to be fine tuned which is given as

$$\zeta' = \zeta + \hat{\theta}. \tag{29}$$

It should be noted that a two-dimensional search (i.e., m and i) is included in the proposed timing function $\Lambda(m,i)$. This is the main difference from the single synchronization point estimation in [14], where only coarse estimation of the packet synchronization point is adopted. The first search parameter is m, corresponding to the first search region in the range around the coarse synchronization point ζ. Meanwhile, the second search parameter is i, corresponding to the range in the region around the tail of the OFDM symbol which yields the expected Doppler shift. Once the fine-tuned ζ' is obtained, the subsequent stage is the estimation of the first order moment $\hat{\phi}$. In existing techniques, [6] and [14], due to the acceleration and the inherent ISI, there is a fluctuation in the maximum of the timing function, and the channel conditions have a direct effect on this maximum. Therefore, centroid-based localization is adopted to estimate $\hat{\phi}$, because it reduces the position uncertainty caused by the fading channel, and the search range is built on the fine-tuned ζ', which can be written as

$$r_D \in \left[\zeta' + N_g + N - \left(\frac{\Upsilon}{2}\right) + i, \zeta' + N - \left(\frac{\Upsilon}{2}\right) + i\right], \tag{30}$$

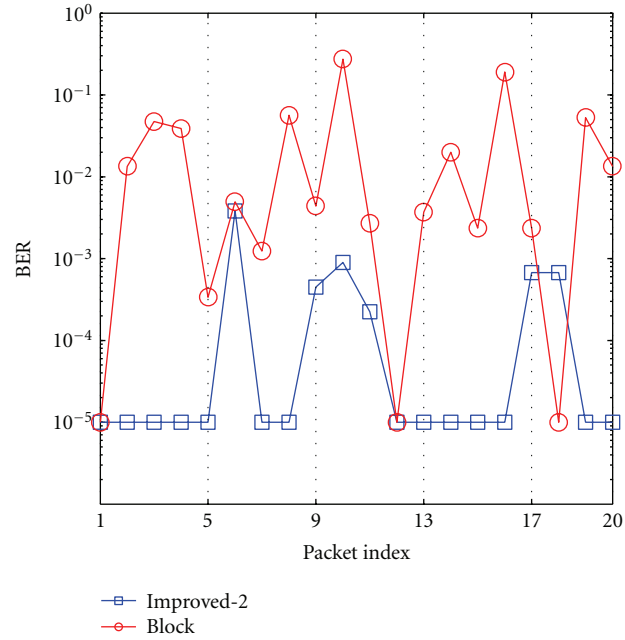

Figure 12: Performance of the proposed system with improved coarse timing estimation.

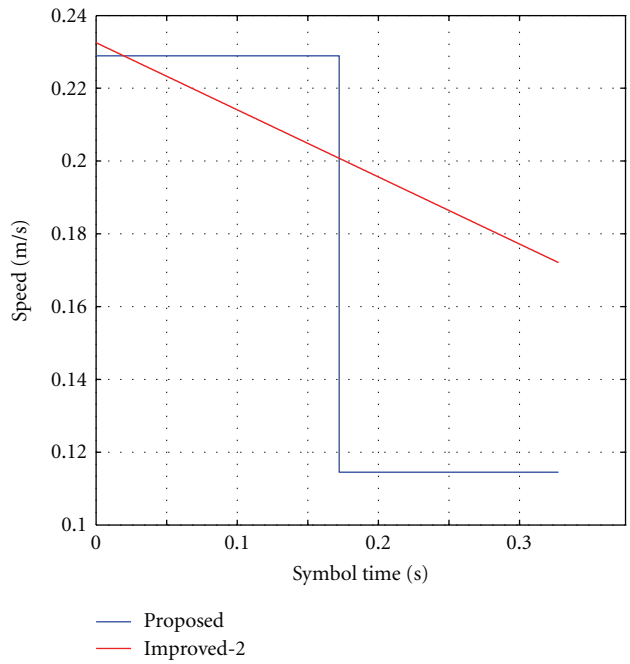

Figure 13: Improved time-varying speed estimation during OFDM symbol 7 of packet 6.

and the centroid-based first order moment $\hat{\phi}_l$ is given as in [14]. Figure 12 shows that fine tuning this parameter results in reducing the BER. It can be inferred from this figure that adjusting the misalignments of the symbol timing due to the time-varying Doppler scale results in an improvement in the reliability of the resampling factor estimation, which in turn reduces the noise that accompanies accumulated errors from symbol to symbol within each packet and ultimately a reduction in BER is obtained.

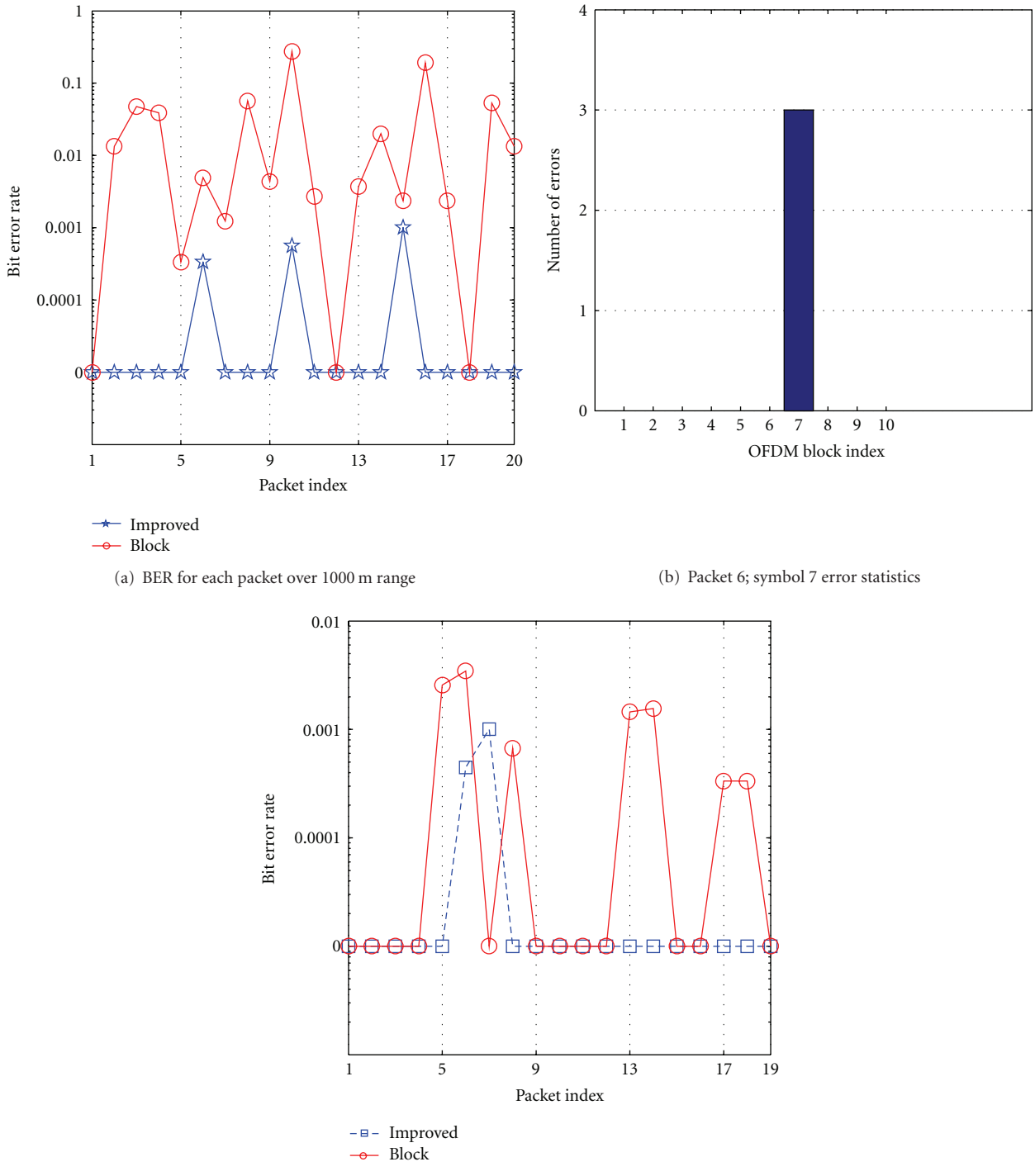

(a) BER for each packet over 1000 m range

(b) Packet 6; symbol 7 error statistics

(c) BER for each packet over 1000 m range at 512 subcarriers

FIGURE 14: Performance of the improved proposed system.

5.4. Performance Evaluation Based on Two-Point Correlation. Fine tuning of the coarse symbol timing facilitates an alternative approach to estimating the first order moment of the correlation lag. The suggested approach here aims to increase the confidence of estimation by considering the first order moment that results from two correlation lags. The first correlation lag is estimated by means of centroid-based localization, in accordance with the anticipated window mentioned earlier. This type of correlation gives an accurate indication of the fractional part of the time-scale expansion/compression. However, the centroid-based localization is severely affected due to the velocity perturbation. This perturbation degrades the estimation performance of the timing function and ultimately $\hat{\phi}_l$. Therefore, an alternative

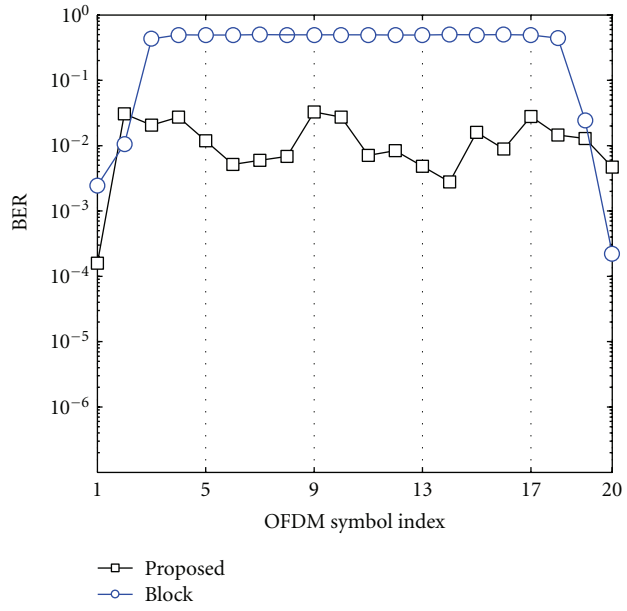

Figure 15: Performance comparison of block-based and proposed techniques.

approach has been adopted by involving another estimation point based upon full cross correlation of the CP with its replica. The addition of this correlation is based on the idea of increasing the certainty of the first order moment estimation. This correlation is based on the assumption that the OFDM timing is approximately aligned due to the fine tuning of the packet synchronization ζ'. By definition, the cross correlation between a pair of energy signals, $x[n]$ and $y[n]$, is given by [25];

$$r_{xy} = \sum_{n=-\infty}^{\infty} x[n]y\left[n-\chi\right], \quad \chi = 0, \pm 1, \pm 2, \ldots, \tag{31}$$

where the parameter χ is called lag and it indicates the time shift between the pair. Based on this theory, the time shift in samples for either expansion or compression can be measured with respect to a reference sequence length of the guard interval N_g. In the case of the existence of Doppler shift, the received samples are shifted to the right in expansion or left for compression with respect to the reference. To be more specific, once the start of the packet ζ is identified, it can be deemed that the symbol timing identification is reliable, and the correlation between the received CP and its replica is computed to measure the time shift in the samples as follows:

$$\Lambda_c \triangleq \left| \sum_{n=0}^{N_g-1} r(\zeta' + n) r\left(\zeta' + n + N - \chi\right) \right|, \quad \chi = 0, \pm 1, \pm 2, \ldots. \tag{32}$$

Considering that the reference sequence of the transmitted CP is $N_{cp}N_s$, the first order moment of the Doppler shift ϕ_x can be approximated as

$$\hat{\phi}_x = \arg\max \Lambda_c - N_{cp}N_s, \quad \chi = 0, \pm 1, \pm 2, \ldots. \tag{33}$$

Adopting such a scenario requires extraction of a fine tuned correlation lag. This necessitates involvement of two parameters of weighting coefficients to perform such a smoothing approach, as mentioned earlier. The coefficients W_1 and W_2 are empirically obtained from the experiment to accommodate the measured channel condition. Therefore, ϕ', which represents the fine tuned first order moment of the correlation lag, is given as

$$\phi' = \hat{\phi}_x W_1 + \hat{\phi}_l W_2. \tag{34}$$

This fine tuned parameter is then delivered to the Doppler extraction in Figure 2(b) in order to estimate the Doppler shift. Accordingly, the estimated Doppler shift, which comprises both an integer and fractional part, is considered and utilized for compensation. Therefore, the estimated resampling factor requires no extraction of the fractional part to estimate the residual Doppler shift, as shown in Figure 2(b); hence, the CFO is approximated as

$$\hat{\epsilon} \simeq 0.5 f_c \delta f / f_s \simeq \frac{\delta f}{8}, \tag{35}$$

where $f_s = 4f_c$. For subcarrier spacing of 3.90625, as in the case of 1024 subcarriers, $\hat{\epsilon}$ is 0.4883 Hz. These two-point estimations of $\hat{\phi}_l$ and $\hat{\phi}_x$, in conjunction with ϕ', contribute towards improving the Doppler shift estimation and thus eliminate the need to determine the CFO. Figure 13 demonstrates the implications of improving the Doppler shift estimation. It is obvious in this figure that there are two estimations that show the deceleration in velocities over the symbol time. With respect to the improved system, the gradient is estimated smoothly. This confirms that an accurate estimation of the drift in samples results in an accurate estimation and tracking of the time-varying Doppler shift. On the other hand, this figure illustrates that perturbations in estimating the variation of speed within the OFDM symbol can lead to inaccurate resampling factor estimation. In particular, it can be inferred from this figure that there is a time-varying Doppler shift during the symbol time which decelerates in the order of 0.25 m/s^2. This deceleration is estimated by smoothing ζ estimation. However, in the proposed system, the deceleration is approximated to 0.48 m/s^2 over the same symbol. For the sake of clarity, the "proposed system" refers to the system before the improvements and the "improved system" refers to the proposed system after improving ζ estimation. Table 2 illustrates the performance comparison between block-based Doppler compensation, time varying Doppler shift compensation, and its improvements. The achieved BER decreases significantly in the proposed system compared with the block-based approach. Likewise, there are additional improvements in the BERs of 83.8% compared with the proposed technique. This is shown in Figure 14(a), where the BER of packet 6 is reduced compared with Figure 8(a). Additionally, the error statistics of packet 6, shown in Figure 8(b) and Figure 14(b), confirm that estimating multilags contributes to an increase in the accuracy of the speed estimation.

As demonstrated in Figure 14(c) and Table 3, the experimental results show that the investigation was also

Table 3: Performance of the experimental results between the improved and block-based Doppler shift techniques for $N_c = 512$.

Packet index	1	2	3	4	5	6	7	8	9	10	11	12	13	14	15	16	17	18	19
Block	0	0	0	0	23	31	0	6	0	0	0	0	13	14	0	0	3	3	0
Improved	0	0	0	0	0	4	9	0	0	0	0	0	0	0	0	0	0	0	0

Table 4: OFDM symbol structure and the corresponding data rates.

N_c	N_d	N_p	N_b	Data rates (kb/s)
512	448	64	20	3.0833
1024	896	128	10	3.2794

Table 5: Complexity estimate.

Operator	Method	
	2D search + centroid	Correlation
+, −	$9\Upsilon' \times W + 8\Upsilon$	$N_g(\log_2 N_g + 1)$
×	$N_g \times \Upsilon 6' \times W + \Upsilon \times N_g$	$3N_g \log_2 N_g$

successful with 512 subcarriers, as it was able to improve performance by about 86%. This was an expected result, because reducing the symbol length entails increasing the subcarrier spacing and reducing the sensitivity to the Doppler shift. Additionally, reducing the symbol length enables more frequent tracking of the Doppler shift. However, severe consequences accompany this reduction in the symbol time, since it mitigates immunity against ISI, in addition to reducing the available bandwidth. This performance reveals that improving the synchronization and adopting smoothing produces low BER. Furthermore, compensating residual Doppler shift or CFO preserves the orthogonality of the subcarriers and ultimately contributes towards mitigating decoding errors. However, it is worthwhile mentioning that this approximation of the CFO cannot be extrapolated to all cases, as in the case of higher acceleration where a special signal processing method, such as an adaptive weighting coefficients selection and/or iterative-based estimation of the Doppler shift, should be adopted due to the effect of the time varying Doppler shift and the inherent ISI on the correlation peak. Another problem with this approach is that it fails to compensate for an abrupt change in the direction of velocity, as it needs at least two symbols to self-adapt to this sudden variation which causes a decoding error.

In terms of the achieved data rate, Table 4 presents two types of OFDM subcarrier allocation that account for the transmission overhead due to pilots, channel coding, and guard period.

Figure 15 shows, in terms of BERs, the performance comparison between the block-based approach and the proposed technique. For the block-based approach, two scenarios of the transmitted packet structure are investigated. The first structure includes 20 ms chirp, followed by a silent period then 10 CP-OFDM symbols. The second structure comprises only a single CP-OFDM frame. The former structure is investigated in the experiment; therefore the second structure is considered here for the purpose of the simulation. It can be seen that the performance of the block approach is poor in the case of multi-scale Doppler within the OFDM symbol. When the speed is low, as shown in the OFDM symbols indices 1 and 20, the block algorithm performance is approximately identical to that of the proposed scheme. However, as the speed increases, the BER also increases in the block-based approach, whereas the proposed algorithm demonstrates less performance error despite an escalation in speed. The degradation in the BERs in the proposed algorithm is due to the effect of the acceleration on the CP correlation.

Additionally, the complexity of the improved algorithm is summarized in Table 5. The complexity estimate includes a two-dimensional (2D) search algorithm mentioned in (32), centroid algorithm in [14], and cross correlation of the received CP samples. In this table, it is shown that the complexity is a linear function of the CP length and the parameters Υ, Υ', and W. It is worth to mention that the correlation complexity estimate is estimated via FFT-based correlation. It can be noticed that no division operation is required. Therefore, in terms of hardware implementation, this Doppler estimate is considered simple.

6. Conclusions

The performance of multi-scale Doppler shift compensation for an OFDM-based UWA communication system has been investigated. The algorithm accommodates for channels with linear acceleration during a packet of multiple OFDM frames. Unlike existing Doppler compensation methods, the proposed scheme is more pragmatic, as it considers the notion that the speed is changing linearly during the OFDM symbol time. Additionally, under the assumption of linear speed during the packet time, it has been shown that using the linear equation approach to predict the first order Doppler shift as a reinforcement parameter leads to acceptable performance over other techniques. Furthermore, it has been shown that employing weighted coefficients improves the performance as it fine tunes the estimated parameters. However, an approach to fine tuning these parameters adaptively and in accordance with the acceleration is required.

References

[1] A. F. Molisch, *Wireless Communications*, John Wiley, New York, NY, USA, 2005.

[2] B. S. Sharif, J. Neasham, O. R. Hinton, and A. E. Adams, "Computationally efficient doppler compensation system for underwater acoustic communications," *IEEE Journal of Oceanic Engineering*, vol. 25, no. 1, pp. 52–61, 2000.

[3] B. S. Sharif, J. Neasham, O. R. Hinton, A. E. Adams, and J. Davies, "Adaptive doppler compensation for coherent acoustic

communication," *IEE Proceedings*, vol. 147, no. 5, pp. 239–246, 2000.

[4] B. Li, S. Zhou, M. Stojanovic, L. L. Freitag, and P. Willett, "Multicarrier communication over underwater acoustic channels with nonuniform doppler shifts," *IEEE Journal of Oceanic Engineering*, vol. 33, no. 2, pp. 198–209, 2008.

[5] S. F. Mason, C. R. Berger, S. Zhou, and P. Willett, "Detection, synchronization, and doppler scale estimation with multicarrier waveforms in underwater acoustic communication," *IEEE Journal on Selected Areas in Communications*, vol. 26, no. 9, pp. 1638–1649, 2008.

[6] J. J. van de Beek, M. Sandell, and P. O. Börjesson, "ML estimation of time and frequency offset in OFDM systems," *IEEE Transactions on Signal Processing*, vol. 45, no. 7, pp. 1800–1805, 1997.

[7] B. C. Kim and I. T. Lu, "Parameter study of OFDM underwater communications system," in *Proceedings of the IEEE Oceans*, vol. 2, pp. 1251–1255, Providence, RI, USA, September 2000.

[8] K. Tu, T. M. Duman, J. G. Proakis, and M. Stojanovic, "Cooperative MIMO-OFDM communications: receiver design for doppler-distorted underwater acoustic channels," in *Proceedings of the 44th Asilomar Conference on Signals, Systems and Computers*, pp. 1335–1339, November 2010.

[9] J. Armstrong, "Analysis of new and existing methods of reducing intercarrier interference due to carrier frequency offset in OFDM," *IEEE Transactions on Communications*, vol. 47, no. 3, pp. 365–369, 1999.

[10] A. F. Molisch, M. Toeltsch, and S. Vermani, "Iterative methods for cancellation of intercarrier interference in OFDM systems," *IEEE Transactions on Vehicular Technology*, vol. 56, no. 4, pp. 2158–2167, 2007.

[11] K. Tu, D. Fertonani, T. M. Duman, M. Stojanovic, J. G. Proakis, and P. Hursky, "Mitigation of intercarrier interference for OFDM over time-varying underwater acoustic channels," *IEEE Journal of Oceanic Engineering*, vol. 36, no. 2, pp. 156–171, 2011.

[12] S. Yerramalli and U. Mitra, "Optimal resampling of OFDMm signals for multiscale-multilag underwater acoustic channels," *IEEE Journal of Oceanic Engineering*, vol. 36, no. 1, pp. 126–138, 2011.

[13] A. E. Abdelkareem, B. S. Sharif, C. C. Tsimenidis, and J. A. Neasham, "Adaptive doppler-shift compensation for OFDM underwater acoustic communications system," in *Proceedings of the Underwater Acoustic Measurements: Technologies and Results (UAM '11)*, Kos, Greece, June 2011.

[14] A. E. Abdelkareem, B. S. Sharif, C. C. Tsimenidis, J. A. Neasham, and O. Hinton, "Low-complexity doppler compensation for OFDM-based underwater acoustic communication systems," in *Proceedings of the IEEE Oceans*, pp. 1–6, Santander, Spain, June 2011.

[15] R. W. Bäuml, R. F. H. Fischer, and J. B. Huber, "Reducing the peak-to-average power ratio of multicarrier modulation by selected mapping," *Electronics Letters*, vol. 32, no. 22, pp. 2056–2057, 1996.

[16] M. Stojanovic, "Low-complexity OFDM detector for underwater channels," in *Proceedings of the MTS/IEEE Ocean Conference*, pp. 18–21, Boston, Mass, USA, September 2006.

[17] B. Li, S. Zhou, M. Stojanovic, L. Freitag, and P. Willett, "Non-uniform doppler compensation for zero-padded OFDM over fast-varying underwater acoustic channels," in *Proceedings of the IEEE Oceans*, pp. 1–6, Aberdeen, UK, June 2007.

[18] M. Speth, S. A. Fechtel, G. Fock, and H. Meyr, "Optimum receiver design for wireless broad-band systems using OFDM-part II," *IEEE Transactions on Communications*, vol. 49, no. 4, pp. 571–578, 2001.

[19] T. Pollet, P. Spruyt, and M. Moeneclaey, "The BER performance of OFDM systems using non-synchronized sampling," in *Proceedings of the Global Telecommunications(GLOBECOM '94)*, vol. 1, pp. 253–257, November 1994.

[20] B. Yang, K. B. Letaief, R. S. Cheng, and Z. Cao, "Timing recovery for OFDM transmission," *IEEE Journal on Selected Areas in Communications*, vol. 49, pp. 467–479, 2000.

[21] M. K. Ozdemir, Logus Broadband, wireless solutions Incorporation, and H. Arslan, "Channel estimation for wireless OFDM systems," *IEEE Communications Surveys and Tutorials*, vol. 9, no. 2, pp. 18–48, 2007.

[22] S. Coleri, M. Ergen, A. Puri, and A. Bahai, "Channel estimation techniques based on pilot arrangement in OFDM systems," *IEEE Transactions on Broadcasting*, vol. 48, no. 3, pp. 223–229, 2002.

[23] M. H. Hsieh and C. H. Wei, "Channel estimation for OFDM systems based on comb-type pilot arrangement in frequency selective fading channels," *IEEE Transactions on Consumer Electronics*, vol. 44, no. 1, pp. 217–225, 1998.

[24] C. P. Shah, C. C. Tsimenidis, B. S. Sharif, and J. A. Neasham, "Low-complexity iterative receiver structure for time-varying frequency-selective shallow underwater acoustic channels using BICM-ID: design and experimental results," *IEEE Journal of Oceanic Engineering*, vol. 36, no. 3, pp. 406–421, 2011.

[25] K. S. Mitra, *Digital Signal Processing A Computer Based Approach*, McGraw-Hill, New York, NY, USA, 2006.